iScience

CellPress
OPEN ACCESS

Article

A descending pathway emanating from the periaqueductal gray mediates the development of cough-like hypersensitivity

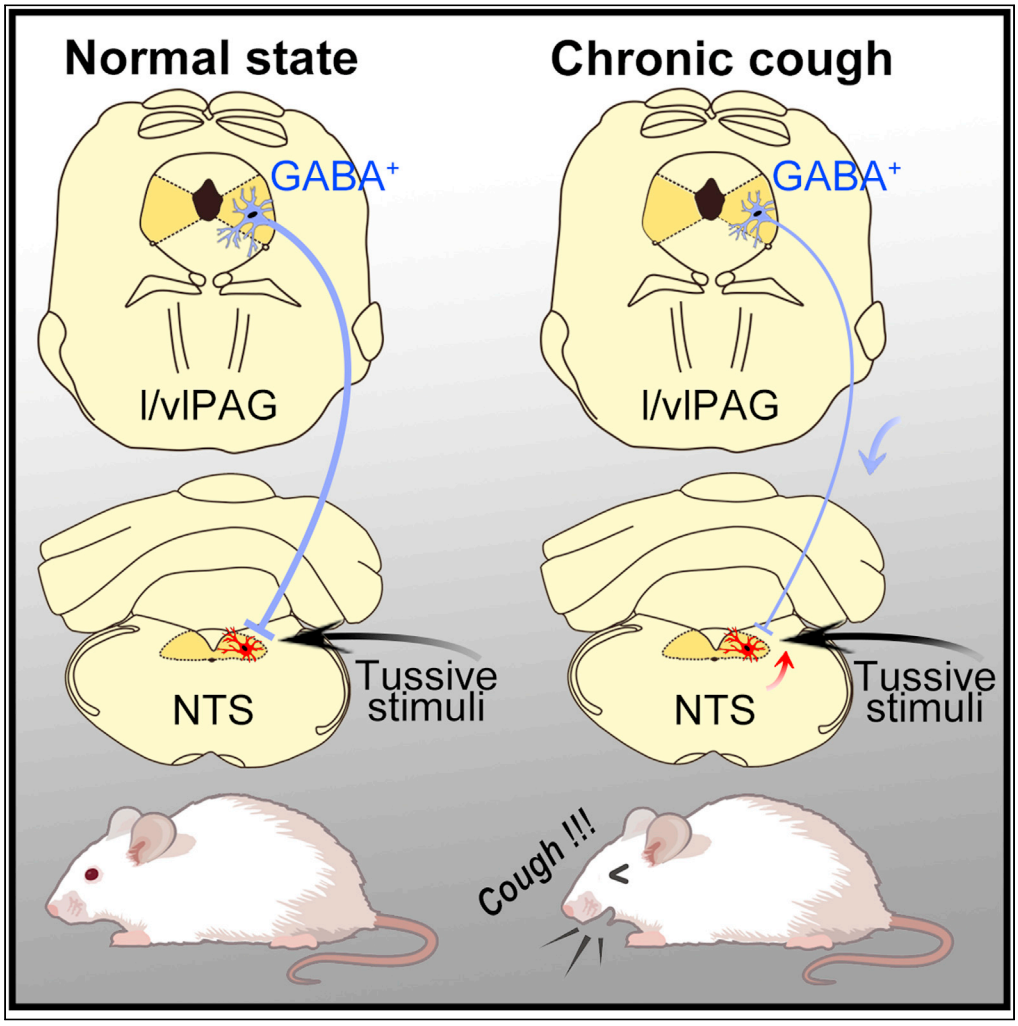

Zhe Chen, Ming-Tong Lin, Chen Zhan, Nan-Shan Zhong, Di Mu, Ke-Fang Lai, Mingzhe J. Liu

dimu08207@ustc.edu (D.M.)
klai@163.com (K.-F.L.)
lmzrondo@ustc.edu (M.J.L.)

Highlights

GABAergic neurons in the l/vlPAG inhibit coughing-like behaviors

The l/vlPAG sends predominately inhibitory projections to the NTS

l/vlPAG GABAergic neurons modulate coughing-like behaviors via descending projections

l/vlPAG-NTS projections mediate cough hypersensitivity via disinhibitory mechanisms

Chen et al., iScience *25*, 103641
January 21, 2022
https://doi.org/10.1016/j.isci.2021.103641

iScience

CellPress
OPEN ACCESS

Article

A descending pathway emanating from the periaqueductal gray mediates the development of cough-like hypersensitivity

Zhe Chen,[1,2,4] Ming-Tong Lin,[1,4] Chen Zhan,[1] Nan-Shan Zhong,[1] Di Mu,[3,*] Ke-Fang Lai,[1,*] and Mingzhe J. Liu[1,5,*]

SUMMARY

Chronic cough is a common refractory symptom of various respiratory diseases. However, the neural mechanisms that modulate the cough sensitivity and mediate chronic cough remain elusive. Here, we report that GABAergic neurons in the lateral/ventrolateral periaqueductal gray (l/vlPAG) suppress cough processing via a descending pathway. We found that l/vlPAG neurons are activated by coughing-like behaviors and that tussive agent-evoked coughing-like behaviors are impaired after activation of l/vlPAG neurons. In addition, we showed that l/vlPAG neurons form inhibitory synapses with the nucleus of the solitary tract (NTS) neurons. The synaptic strength of these inhibitory projections is weaker in cough hypersensitivity model mice than in naïve mice. Important, activation of l/vlPAG GABAergic neurons projecting to the NTS decreases coughing-like behaviors. In contrast, suppressing these neurons enhances cough sensitivity. These results support the notion that l/vlPAG GABAergic neurons play important roles in cough hypersensitivity and chronic cough through disinhibition of cough processing at the medullary level.

INTRODUCTION

Cough is the most common symptom in respiratory outpatients, one-third of whom are patients with chronic cough (Morice et al., 2019). Cough can in turn cause cough hypersensitivity, depression, anxiety, or insomnia in patients with chronic cough (Everett et al., 2007; Ovsyannikov et al., 2019). Chronic cough is widely considered a cough hypersensitivity syndrome and is characterized by coughing in response to low-intensity airway stimulation (Morice et al., 2014). Previous studies have shown that cough hypersensitivity is likely mediated by both the peripheral and central nervous systems (Ando et al., 2016; Singh et al., 2020). However, little is known about the central cellular and circuit mechanisms underlying the modulation of cough sensitivity.

Recently, several regions of the brain that may regulate cough sensitivity were identified by functional magnetic resonance imaging studies (Ando et al., 2016; Bautista et al., 2019). Patients with cough hypersensitivity exhibited an elevated neural activity in the lateral/ventrolateral periaqueductal gray (l/vlPAG) and nucleus of the solitary tract (NTS) when exposed to nebulized capsaicin (Ando et al., 2016; McGovern et al., 2017). In addition, it has been found that the l/vlPAG is involved in controlling the respiratory functions and that electric stimulation of periaqueductal gray decreases coughing reflexes (Faull et al., 2019). It has been shown that l/vlPAG subpopulations and their descending pathways are critical for itch and pain processing (Gao et al., 2019; Samineni et al., 2017, 2019; Liu et al., 2019), the anatomical basis and molecular mechanisms of which are similar to that of cough processing to a certain degree, given that they can all be mediated by small-diameter sensory C-fibers, TRP (transient receptor potential) superfamily ionotropic receptors and inflammatory mediators (Lavinka and Dong, 2013; McGovern et al., 2017; Pecova et al., 2020). Activation of l/vlPAG GABAergic neurons suppresses itch but facilitates pain behaviors, whereas inhibition of these neurons results in enhanced itch and decreased pain behaviors, indicating that these neurons play a role in gating itch processing and promoting pain processing (Samineni et al., 2017, 2019). Moreover, activation of l/vlPAG glutamatergic neurons results in increased itch and decreased pain behaviors, whereas inhibition of these neurons alleviates itch and potentiates pain behaviors (Samineni et al., 2017, 2019). A recent study suggested that l/vlPAG tachykinin 1-expressing neurons, a subgroup of l/vlPAG glutamatergic neurons, facilitate itch but not pain signal processing, suggesting complicated roles of l/vlPAG

[1]State Key Laboratory of Respiratory Disease, Guangdong-Hong Kong-Macao Joint Laboratory of Respiratory Infectious Disease, National Clinical Research Center for Respiratory Disease, Guangzhou Institute of Respiratory Health, The First Affiliated Hospital of Guangzhou Medical University, 151 Yan Jiang Xi Road, Guangzhou 510120, China

[2]Laboratory of Cough, Affiliated Kunshan Hospital of Jiangsu University, Suzhou, Jiangsu 215300, China

[3]Department of Anesthesiology, Shanghai General Hospital, Shanghai Jiao Tong University School of Medicine, No. 650 Xin Song Jiang Road, Shanghai 201620, China

[4]These authors contributed equally

[5]Lead contact

*Correspondence: dimu08207@ustc.edu (D.M.), klai@163.com (K.-F.L.), lmzrondo@ustc.edu (M.J.L.)

https://doi.org/10.1016/j.isci.2021.103641

glutamatergic neurons in regulating somatosensory processing (Gao et al., 2019). However, it remains unknown whether and how neuronal subpopulations in the l/vlPAG modulate cough sensitivity.

In addition to the l/vlPAG, the NTS might also be involved in the modulation of cough sensitivity (Mazzone et al., 2015; McGovern et al., 2017; Singh et al., 2020). The NTS receives projections from nodose sensory neurons, which primarily innervate the intrapulmonary airways (Mazzone and Undem, 2016; McGovern et al., 2015a). Many studies have started to dissect the functional role of the NTS in regulating cough sensitivity (Cinelli et al., 2016; Gestreau et al., 1997; Haji et al., 2012; Jakus et al., 2008; Mutolo et al., 2007, 2008). Several studies have reported that neurons in the NTS are activated by the airway stimulation-induced coughing reflex (Gestreau et al., 1997; Haji et al., 2012; Jakus et al., 2008). It has been shown that some antitussive agents suppress coughing behavior via suppression of NTS neurons (Gestreau et al., 1997; Mutolo et al., 2008). Moreover, activation or disinhibition of NTS neurons by microinjection of drugs promotes cough processing (Cinelli et al., 2016; Mutolo et al., 2007). Our recent study further demonstrated that neuronal hyperexcitability in the NTS might be involved in chronic cough (Chen et al., 2019). In addition, NTS neurons receiving projections from the airway send projections to many sensation-related brain regions, including the locus coeruleus, parabrachial nuclei, thalamus, and central amygdala (McGovern et al., 2015a, 2015b). Given that the NTS receives projections from l/vlPAG neurons (Farkas et al., 1997; Gasparini et al., 2020), it remains to be determined whether the l/vlPAG-NTS circuit modulates cough sensitivity.

Here, we revealed the central cellular and circuit mechanisms underlying the modulation of cough sensitivity by combining electrophysiological, optogenetic, and pharmacogenetic approaches. We also dissected the distinct roles of l/vlPAG subpopulations that are critical for mediating cough hypersensitivity via descending projections.

RESULTS

Establishment of a cough-like model in mice

Most previous studies used the guinea pig as an animal model in monitoring cough reflexes (Driessen et al., 2020; Ruhl et al., 2020; Yu et al., 2021). However, many new useful tools, such as pharmacogenetics, optogenetics, and fiber photometry, are difficult to use on guinea pigs owing to the lack of transgenic guinea pig models expressing cell type-specific Cre-recombinase. Therefore, to take advantage of these useful techniques to dissect more cellular and neural mechanisms underlying the regulation of cough sensitivity, we developed a coughing-like model in freely moving mice (Figure 1A). Citric acid (CA) and capsaicin are the most widely used tussive agents triggering cough reflexes (Morice et al., 2007). After introducing aerosolized CA or capsaicin solution via a nebulizer to the chambers, mice exhibited coughing-like responses evoked by either of these two tussive agents (Figures 1B–1D; Video S1). Besides the coughing-like responses, eupnea responses and baseline respiratory parameters were also monitored (Figure 1B and S1). Whole-body plethysmography (WBP) showed coughing-like respiratory patterns characterized by an inspiration phase, followed by a compression phase and a strong expiration phase (Figure 1B). Respiratory patterns are correlated well with audio signals, simultaneously monitored by the WBP and a microphone (Figure 1B). Some (nearly 15%) recorded responses are hardly distinguished between coughing-like and expiration reflexes without the inspiration phases (Lin et al., 2017), so we counted them together in the evaluation of coughing-like responses. Given that cough signals are initiated in airways and lungs innervated by the cervical vagus nerve and that sneeze signals are initiated in the nasal mucosa innervated by the anterior ethmoidal nerve (AEN) (Batsel and Lines, 1978; Li et al., 2021; Polverino et al., 2012), to confirm the monitored coughing-like respiratory patterns are coughs but not sneezes, which could also be triggered by capsaicin (Li et al., 2021), we performed a unilateral cervical vagotomy (UCV) or an AEN transection on naïve mice. After UCV, the number of coughing-like responses evoked by CA or capsaicin was significantly reduced, whereas the number of coughing-like responses were unchanged after transecting AEN (Figures 1C and 1D), indicating that these responses are coughs mediated by the cervical vagus nerve but not the AEN. In addition, the number of sneezing-like responses evoked by CA or capsaicin was significantly reduced after transecting AEN (Figure 1E), suggesting the success of AEN transection. Therefore, our studies fully developed the mouse cough-like model.

Activation of neurons in the l/vlPAG suppressed tussive agent-evoked coughing-like behaviors

Because previous studies have indicated that the l/vlPAG is activated by airway stimulation with inhaled capsaicin (Ando et al., 2016), we first examined the involvement of l/vlPAG in airway stimulation-induced

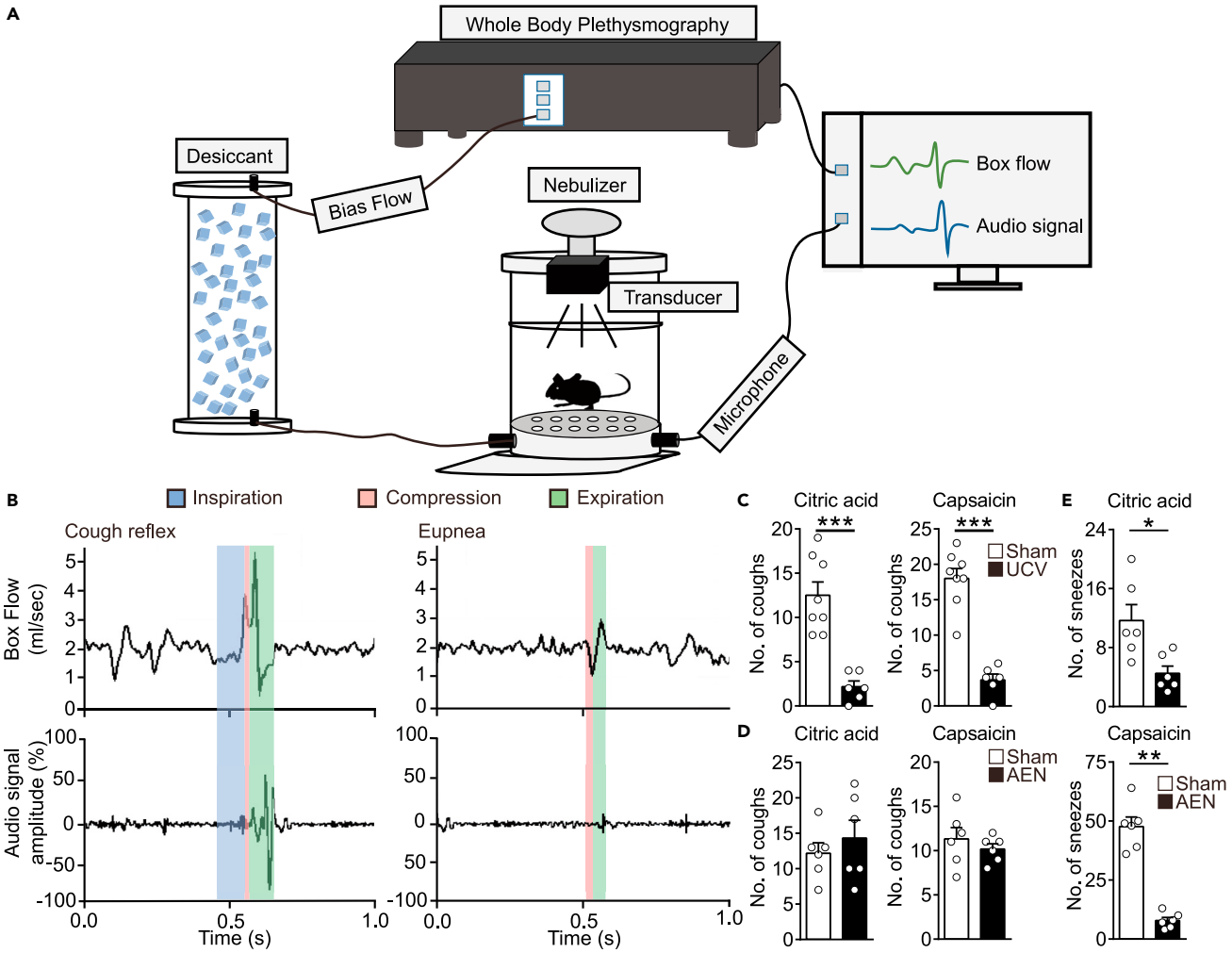

Figure 1. Developing the mouse cough-like model

(A) Schematic diagram of the experimental establishment.

(B) Representative traces showing the simultaneous WBP box flow and audio signal recordings generated by a single cough (left) and a single expiration reflex (right) of a freely moving WT mouse upon exposure to nebulized citric acid solution (0.4 M).

(C) The UCV, which blocks airway and lung sensation transmitting to the central nervous systems, significantly reduced coughing-like behaviors evoked by nebulized CA (0.4 M) or capsaicin (10 μM) solution, Mann-Whitney test (n = 6 or 8 mice).

(D and E) AEN transection, which blocks nasal mucosa sensation transmitting to the central nervous system, significantly reduced sneezing-like but not coughing-like behaviors evoked by nebulized CA (0.4 M) or capsaicin (10 μM) solution, Mann-Whitney test (n = 6 mice).All error bars represent the SEMs. *p <0.05, **p <0.01, ***p <0.001.

coughing-like behavior. We found that the number of c-Fos$^+$ neurons in the l/vlPAG of mice was markedly increased after inhalation of the nebulized tussive agents CA and capsaicin (Figures 2A–2C), suggesting that the neurons in the l/vlPAG of mice are activated by airway stimulation with inhaled CA or capsaicin.

To investigate whether the elevation of l/vlPAG activity is the cause or an effect of airway stimulation-induced coughing-like behavior, we bilaterally injected an adeno-associated virus (AAV) expressing hM3Dq, a designer receptor exclusively activated by designer drugs (DREADD) (Urban and Roth, 2015a), into the l/vlPAG of wild-type (WT) mice. This led to the local expression of hM3Dq in the l/vlPAG. The control group was injected with AAV-hSyn-mCherry (Figures 2D and 2E). Behavioral experiments were performed 2–3 weeks after AAV injection. The mice were injected intraperitoneally (i.p.) with clozapine-N-oxide (CNO) 30–40 min before inhaling the nebulized tussive agents. We found that pharmacogenetic activation of l/vlPAG neurons largely decreased the coughing-like behavior evoked by inhalation of CA (Figure 2F). Consistently, the same manipulation also significantly decreased the number of coughing-like behaviors induced by capsaicin (Figure 2G). Activation of

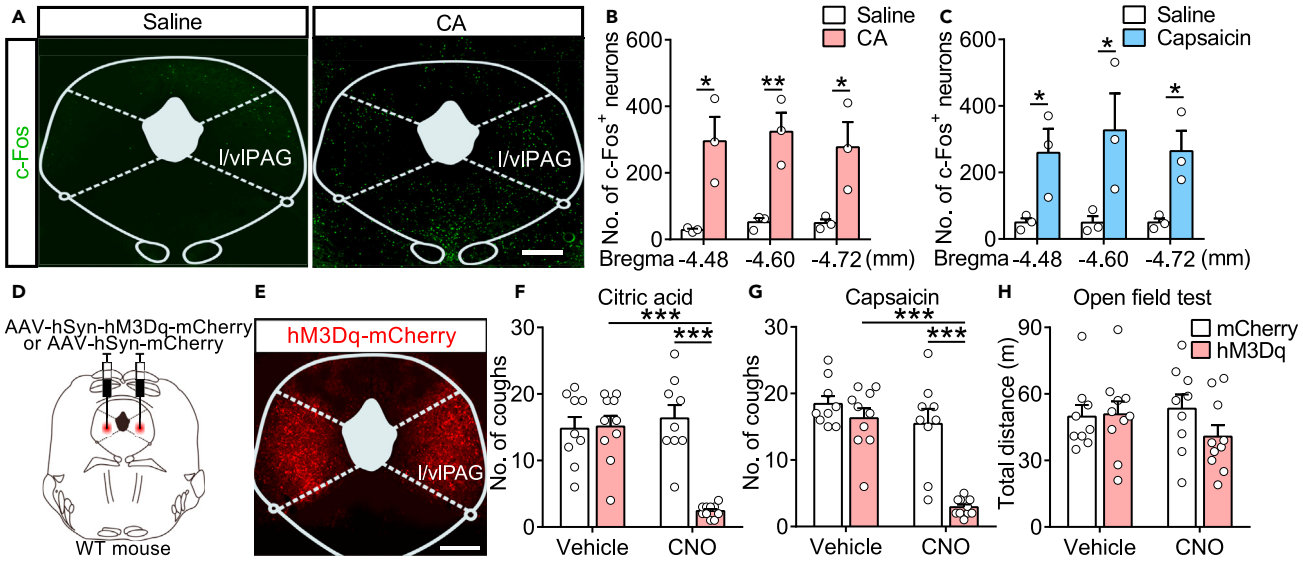

Figure 2. Pharmacogenetic activation of l/vlPAG neurons attenuates coughing-like behaviors

(A) c-Fos expression in the l/vlPAG in response to nebulized saline (left) or CA (right). Scale bar, 300 μm.

(B and C) Number of c-Fos$^+$ neurons in different parts of the l/vlPAG in the groups treated with nebulized CA (B) or capsaicin (C) compared with the control group, unpaired t test (n = 3 mice).

(D) A schematic diagram showing the sites of AAV-hSyn-hM3Dq-mCherry or AAV-hSyn-mCherry virus injection into the bilateral l/vlPAG of WT mice.

(E) The expression of hM3Dq-mCherry in the l/vlPAG. Scale bar, 300 μm.

(F and G) The effects of pharmacogenetic activation of l/vlPAG neurons by injection of CNO (1 mg/kg, i.p.) on coughing-like behaviors induced by nebulized CA (F) or capsaicin (G), two-way ANOVA (n = 9 or 10 mice).

(H) The effects of pharmacogenetic activation of l/vlPAG neurons by injection of CNO (1 mg/kg, i.p.) on locomotion, two-way ANOVA (n = 9 or 10 mice). All error bars represent the SEMs. *p <0.05, **p <0.01, ***p <0.001.

l/vlPAG neurons did not significantly affect the locomotor activity of mice (Figure 2H), excluding the possibility that changes in locomotion affected coughing-like behavior. These results suggested that neurons in the l/vlPAG play a functional role in decreasing cough sensitivity.

To further demonstrate the role of l/vlPAG neurons in modulating cough sensitivity under physiological conditions, we examined the effect of l/vlPAG neuron suppression on cough sensitivity using a method involving a DREADD (Armbruster et al., 2007; Urban and Roth, 2015b). We bilaterally injected AAV-hSyn-hM4Di-mCherry or AAV-hSyn-mCherry into the l/vlPAG of WT mice (Figures S2A and S2B). We found that inhibition of l/vlPAG neurons significantly increased the number of coughing-like behaviors induced by inhalation of CA, capsaicin, or saline in mice (Figures S2C–S2E). Inhibition of l/vlPAG neurons did not affect the locomotion of mice (Figure S2F). Taken together, these findings confirmed that the l/vlPAG plays a critical role in modulating cough sensitivity.

Functional role of l/vlPAG GABAergic neurons in cough sensitivity

Some subtypes of neurons in the l/vlPAG have been identified (Gao et al., 2019; Samineni et al., 2017, 2019). The l/vlPAG GABAergic neurons have been shown to modulate pain and itch processing (Samineni et al., 2017, 2019). However, the functional role of l/vlPAG GABAergic neurons in cough sensitivity remains unclear. We examined the role of l/vlPAG GABAergic neurons in modulating tussive agent-evoked coughing-like behavior. We first injected AAV-DIO-hM3Dq-mCherry into the l/vlPAG of *Vgat-Cre* mice, and AAV-DIO-mCherry was injected as a control (Figures 3A, 3B and S3A–S3C). In the behavioral test, animals from both groups were injected with saline or CNO (i.p.) 30–40 min before inhalation of nebulized CA, capsaicin, or saline. We found that pharmacogenetic activation of l/vlPAG GABAergic neurons significantly suppressed coughing-like behavior evoked by CA, capsaicin, and saline (Figures 3C–3E). Activation of the l/vlPAG GABAergic neurons did not significantly affect the locomotion (Figure 3F). To determine whether inhibition of l/vlPAG GABAergic neurons also affects the cough sensitivity, we expressed hM4Di in l/vlPAG GABAergic neurons and assessed cough behavior 3 weeks later (Figures 3G, 3H, and S3D–S3F). We found that pharmacogenetic suppression of l/vlPAG GABAergic neurons significantly enhanced the number of

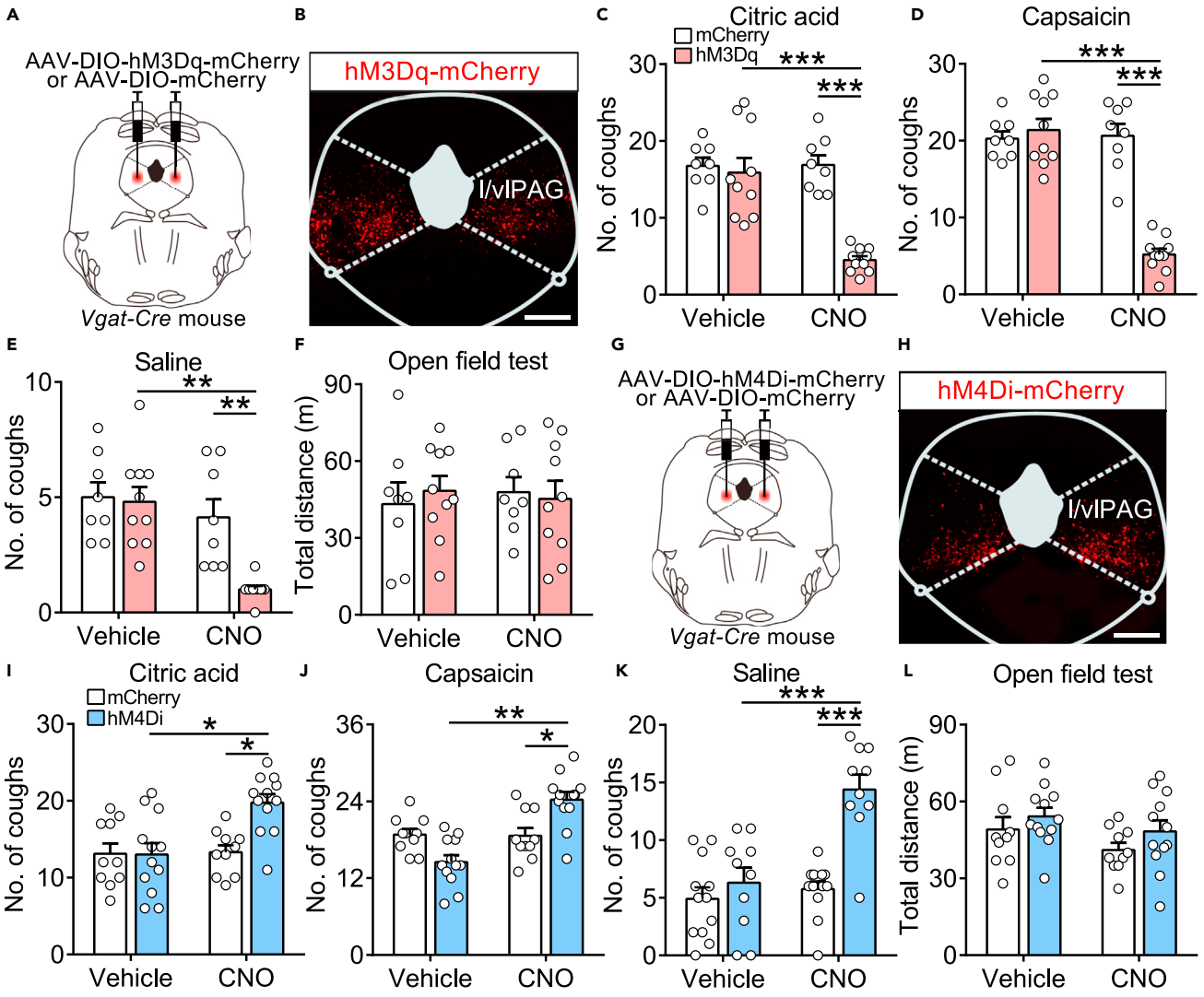

Figure 3. Pharmacogenetic manipulation of l/vlPAG GABAergic neurons modulates cough sensitivity

(A) A schematic diagram showing the sites of AAV-DIO-hM3Dq-mCherry or AAV-DIO-mCherry virus injection into the bilateral l/vlPAG of Vgat-Cre mice.

(B) Expression of hM3Dq-mCherry in the l/vlPAG. Scale bar, 300 μm.

(C–E) Effects of pharmacogenetic activation of GABAergic neurons in the l/vlPAG by injection of CNO (1 mg/kg, i.p.) on coughing-like behaviors induced by nebulized CA (C), capsaicin (D), or saline (E); two-way ANOVA (n = 8 or 10 mice).

(F) Effects of pharmacogenetic activation of GABAergic neurons in the l/vlPAG by injection of CNO (1 mg/kg, i.p.) on locomotion; two-way ANOVA (n = 8 or 10 mice).

(G) A schematic diagram showing the sites of AAV-DIO-hM4Di-mCherry or AAV-DIO-mCherry virus injection into the bilateral l/vlPAG of Vgat-Cre mice.

(H) Expression of hM4Di-mCherry in the l/vlPAG. Scale bar, 300 μm.

(I–K) Effects of pharmacogenetic inhibition of GABAergic neurons in the l/vlPAG by injection of CNO (1 mg/kg, i.p.) on coughing-like behaviors induced by nebulized CA (I), capsaicin (J), or saline (K);, two-way ANOVA (n = 10 or 12 mice).

(L) Effects of pharmacogenetic activation of GABAergic neurons in the l/vlPAG by injection of CNO (1 mg/kg, i.p.) on locomotion; two-way ANOVA (n = 10 or 12 mice). All error bars represent the SEMs. *p <0.05, **p <0.01, ***p <0.001.

cough reflex behaviors in mice without affecting locomotion (Figures 3I–3L). These results supported the idea that l/vlPAG GABAergic neurons play a critical role in dynamically modulating cough sensitivity.

Functional projections from the l/vlPAG to the NTS

Next, we investigated how l/vlPAG neurons control cough sensitivity. Previous studies have indicated that the l/vlPAG modulates somatosensory signal processing via descending projections (Gao et al., 2019). The

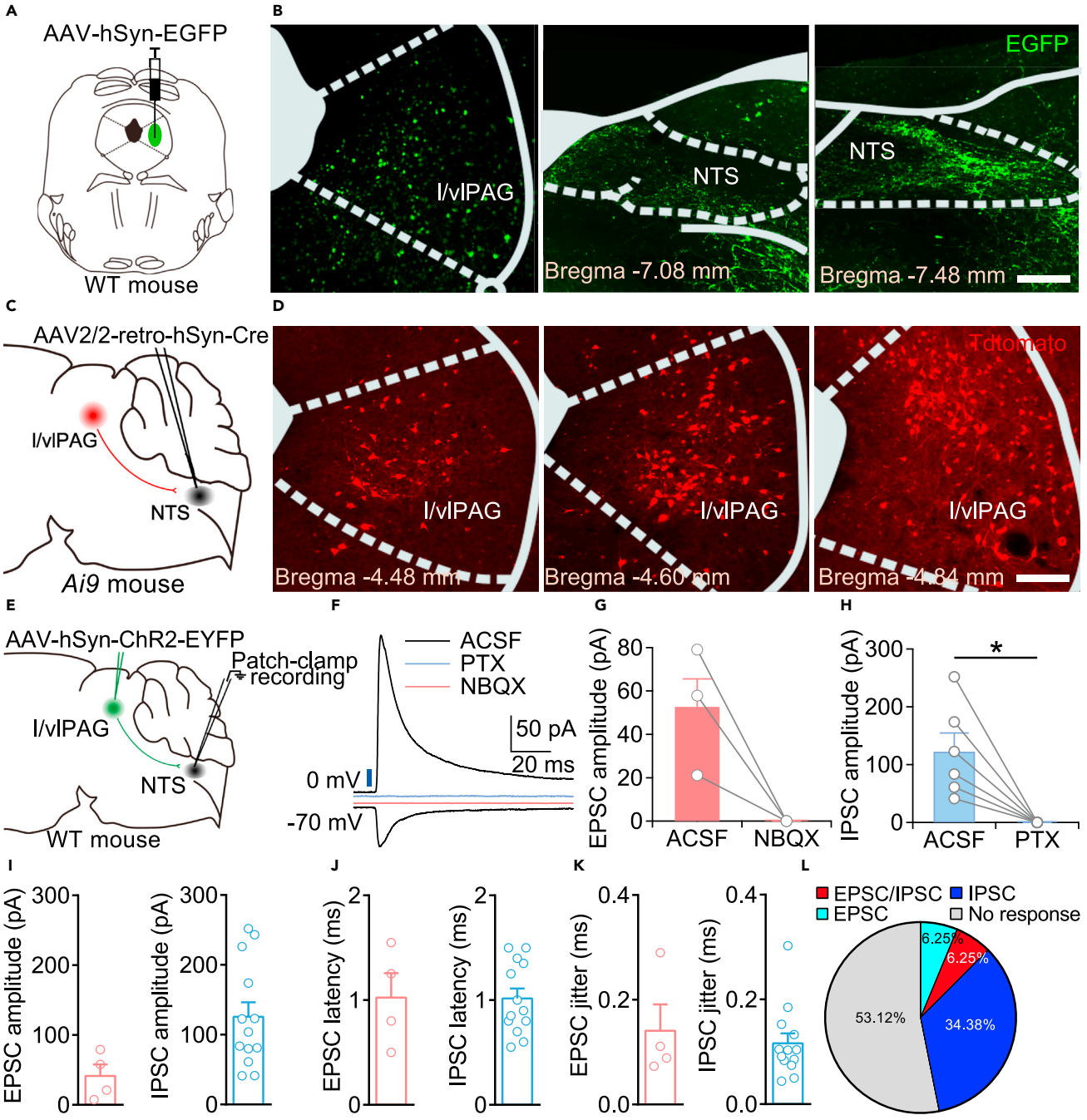

Figure 4. Synaptic inputs from the l/vlPAG to NTS neurons

(A) Schematic showing the site of AAV-hSyn-EGFP injection into the unilateral l/vlPAG of WT mice.

(B) Images showing EGFP expression in the l/vlPAG (left) and the NTS (middle and right). Scale bars, 200 μm.

(C) Schematic showing the site of AAV2/2-retro-hSyn-Cre injection into the unilateral NTS of Ai9 mice.

(D) Images showing tdTomato expression in different parts of the l/vlPAG. Scale bars, 300 μm.

(E) Schematic showing the site of AAV-hSyn-ChR2-EYFP injection into the unilateral l/vlPAG of WT mice and patch-clamp recording of NTS neurons.

(F) Responses evoked by photostimulation of l/vlPAG ChR2$^+$ fibers in an NTS neuron in ACSF (black) and in the presence of picrotoxin (PTX; 50 μM; blue) or NBQX (10 μM; red). Blue bar, LED stimulation (475 nm, 1 ms).

(G) Summary data of the amplitude of EPSCs recorded in NTS neurons evoked by photostimulation of l/vlPAG ChR2$^+$ fibers before and after the application of NBQX (n = 3 neurons from 3 mice), Wilcoxon signed-rank test.

(H) Summary data of the amplitude of IPSCs recorded in NTS neurons evoked by photostimulation of l/vlPAG ChR2$^+$ fibers before and after the application of PTX (n = 6 neurons from 6 mice), Wilcoxon signed-rank test. *p <0.05.

Figure 4. *Continued*

(I) Summary data of the amplitudes of light-evoked EPSCs (4/32 neurons) and IPSCs (13/32 neurons) in NTS neurons evoked by photostimulation of l/vlPAG ChR2$^+$ fibers.

(J) Summary data of the latencies of light-evoked EPSCs and IPSCs in NTS neurons.

(K) Summary data of the jitters of light-evoked EPSCs and IPSCs in NTS neurons.

(L) The connectivity of NTS neurons receiving different inputs from the l/vlPAG is shown. All error bars represent the SEMs.

NTS is a well-known hub that modulates the cough reflex and airway sensory processing (Singh et al., 2020). In addition, the NTS is known to receive projections from the l/vlPAG (Farkas et al., 1997; Gasparini et al., 2020). However, whether these connections regulate cough sensitivity and how they process airway sensory signals remain unclear. Therefore, the anatomical and functional connections between the l/vlPAG and the NTS and the roles of these connections in cough regulation were examined.

First, to confirm the existence of projections from the l/vlPAG to the NTS, we unilaterally injected AAV-hSyn-EGFP into the l/vlPAG of WT mice and then examined EGFP expression in the NTS (Figure 4A). Dense EGFP$^+$ fibers were observed in the NTS (Figure 4B). The existence of l/vlPAG-NTS projections was further confirmed by an AAV-based retrograde labeling technique (Tervo et al., 2016). AAV2/2-retro-hSyn-Cre was unilaterally injected into the NTS of *Ai9* mice and numerous tdTomato$^+$ neurons were observed in the l/vlPAG (Figures 4C and 4D), indicating that l/vlPAG neurons send axons to the NTS.

To further examine the identity of functional projections from the l/vlPAG to the NTS, we injected AAV-hSyn-ChR2-EYFP into the l/vlPAG of WT mice and obtained whole-cell patch-clamp recordings from neurons in NTS slices (Figure 4E). We found that photostimulation of ChR2$^+$ fibers originating in the l/vlPAG evoked predominately inhibitory postsynaptic currents (IPSCs) with small excitatory postsynaptic current (EPSC) components in NTS neurons (Figures 4F–4L). Light-evoked EPSCs were blocked by bath application of the AMPA receptor antagonist 2,3-dihydroxy-6-nitro-7-sulfamoyl-benzo(f)quinoxaline (NBQX), and light-evoked IPSCs were blocked by bath application of the $GABA_A$ receptor antagonist picrotoxin (PTX; Figures 4G and 4H). The latency of light-evoked EPSCs and IPSCs was ~1.0 ms (Figure 4J), indicating a monosynaptic connection between l/vlPAG and NTS neurons. We also analyzed the latency jitter of these recorded neurons, and we found that most of the neurons had a jitter of less than 0.2 ms (Figure 4K), which is consistent with a monosynaptic connection. Thus, l/vlPAG neurons form dominant direct inhibitory connections with the NTS neurons.

Role of l/vlPAG-NTS connections in cough sensitivity

As the majority of l/vlPAG-NTS projections are GABAergic, we examined the function of the inhibitory projections first. We hypothesized that l/vlPAG GABAergic neurons modulate the cough sensitivity via the NTS. If this is true, then specific activation of l/vlPAG GABAergic neurons projecting to the NTS would also suppress coughing-like behavior. We used a retrograde labeling technique combined with a dual-recombinase system (Li et al., 2018). AAV2/2-retro-FLEX-Flpo was bilaterally injected into the NTS, and AAV-fDIO-hM3Dq-mCherry or AAV-fDIO-mGFP was injected into the l/vlPAG of *Vgat-Cre* mice (Figure 5A). The expression of hM3Dq was dependent on both Cre and Flpo recombinase; therefore, only GABAergic neurons projecting to the NTS expressed hM3Dq (Figures 5B and S4). It was found that activation of l/vlPAG GABAergic neurons projecting to the NTS with CNO (i.p., 1 mg/kg) inhibited the coughing-like behaviors but not the locomotion of mice (Figures 5C–5F, S5A, and S5B). Whether the expression of an inhibitory DREADD in the l/vlPAG-NTS projections enhanced cough responses was also examined (Figures 5G and 5H). As expected, delivery of CNO (i.p., 1 mg/kg) significantly increased the number of coughing-like behaviors in mice treated with nebulized CA, capsaicin, or saline without affecting the locomotion (Figures 5I–5L, S5C, and S5D). These data indicated that l/vlPAG-NTS inhibitory projections decrease cough sensitivity, consistent with the behavior observed after activation of the l/vlPAG GABAergic neurons (Figures 3A–3F).

Furthermore, we investigated the role of glutamatergic l/vlPAG–NTS projections via the same manipulation in *Vglut2-Cre* mice. We found that pharmacogenetic activation or suppression of l/vlPAG glutamatergic neurons projecting to the NTS did not affect the coughing-like behaviors or locomotion of mice (Figure S6), indicating that weak excitatory l/vlPAG-NTS projections are not involved in cough sensitivity regulation. Taken together, these findings suggested that l/vlPAG GABAergic neurons projecting to the NTS play a crucial role in modulating the cough sensitivity of mice.

Disinhibition of the l/vlPAG-NTS circuit in a mouse model of chronic cough

It is generally believed that cough hypersensitivity underlies the development of chronic cough in the majority of patients (Morice et al., 2014). Therefore, to assess the possible role of the l/vlPAG-NTS circuit in chronic cough, we used the repeated airway stimulation-induced cough hypersensitivity mouse model, which mimics a guinea pig model of cough hypersensitivity (Nakaji et al., 2016). Mice inhaled nebulized CA or saline 4 h a day (Figure 6A). After 14 days of inhalation, the mice treated with CA displayed cough hypersensitivity in routine assays, including more CA- or capsaicin-induced coughs and more spontaneous coughing-like reflexes than the control mice (Figures 6B–6E). These results suggested that cough hypersensitivity is reliably induced by 14-day CA exposure.

To examine the change in GABAergic l/vlPAG-NTS projections in the cough hypersensitivity mouse model, we performed slice electrophysiology combined with optogenetics. We injected AAV-hSyn-ChR2-EYFP into the l/vlPAG of WT mice and treated these mice with nebulized CA or saline for 14 days. Then, we obtained whole-cell patch-clamp recordings from NTS neurons in slices (Figure 6F). We found that photostimulation of $ChR2^+$ fibers originating in the l/vlPAG evoked smaller IPSCs in NTS neurons in mice treated with CA than those treated with saline (Figures 6G and 6H). We also calculated the paired-pulse ratio (PPR), which is related to the probability of vesicle release, of each recorded NTS neuron (Silver et al., 1998). NTS neurons in mice exposed to saline exhibited paired-pulse depression to a similar degree, and the majority of NTS neurons in mice treated with CA showed paired-pulse facilitation (Figures 6G and 6I). This indicated that GABAergic l/vlPAG-NTS axons had a relatively low probability of transmitter release, meaning that GABAergic synapse strength was significantly weaker and that the inhibitory control of NTS neurons was diminished in the cough hypersensitivity model mice.

If NTS neurons are mainly inhibited by l/vlPAG GABAergic inputs, a decrease in inhibitory inputs under chronic cough conditions should result in disinhibition of NTS neurons. To further determine whether loss of inhibitory control of the NTS by the l/vlPAG can induce hyperexcitability of NTS neurons, we recorded NTS neurons in slices from cough hypersensitivity model mice (Figures 6J and 6K). We found an increase in the number of spikes in NTS neurons in mice exposed to CA compared with control mice (Figures 6L and 6M), suggesting that NTS neuronal activity is increased in cough hypersensitivity model mice.

To further investigate the necessity of NTS neuronal hyperexcitability in cough hypersensitivity, we selectively inhibited NTS neurons by introducing the inhibitory molecule hM4Di into the NTS and i.p. injecting mice with CNO (Figures 6N and 6O). We found that pharmacogenetic suppression of NTS neurons significantly decreased coughing-like behaviors in cough hypersensitivity model mice (Figures 6P and 6Q). Taken together, these findings indicated that repeated airway stimulation with CA induces disinhibition of l/vlPAG-NTS projections, leading to NTS neuronal hyperexcitability, which results in cough hypersensitivity in mice.

DISCUSSION

In this study, we demonstrated the descending regulatory action of l/vlPAG neurons in cough sensitivity and determined the subtype of l/vlPAG neurons that regulate cough-related neural processing at the medullary level. We found that the l/vlPAG is activated by the coughing-like reflex and global activation of l/vlPAG neurons suppresses coughing-like behaviors. In addition, we found that l/vlPAG GABAergic neurons form inhibitory synapses with NTS neurons and play an essential role in gating the cough-related neural pathway.

Establishment of a mouse cough-like model

For investigating the pathological mechanisms underlying cough, many kinds of animals have been utilized, including guinea pigs, cats, dogs, and pigs (Bolser, 2004). However, to examine the more precise evidence for the development of chronic cough, we should take advantage of some newly developed techniques, which are not fully optimized on those animals but are wildly used in mice (Nectow and Nestler, 2020). Therefore, to determine the cellular and circuit mechanisms modulating cough sensitivity, we developed a mouse cough-like model combining the WBP and audio signal recording. Cough responses evoked by CA, capsaicin, or saline could be successfully monitored, the waves of which are similar to the cough responses evoked by NH_3 and SO_2 monitored by another system (Lin et al., 2017; Zhang et al., 2017). Another study also monitored capsaicin-evoked coughing-like responses by WBP and audio signal recording (Chen et al., 2013), the waves of which

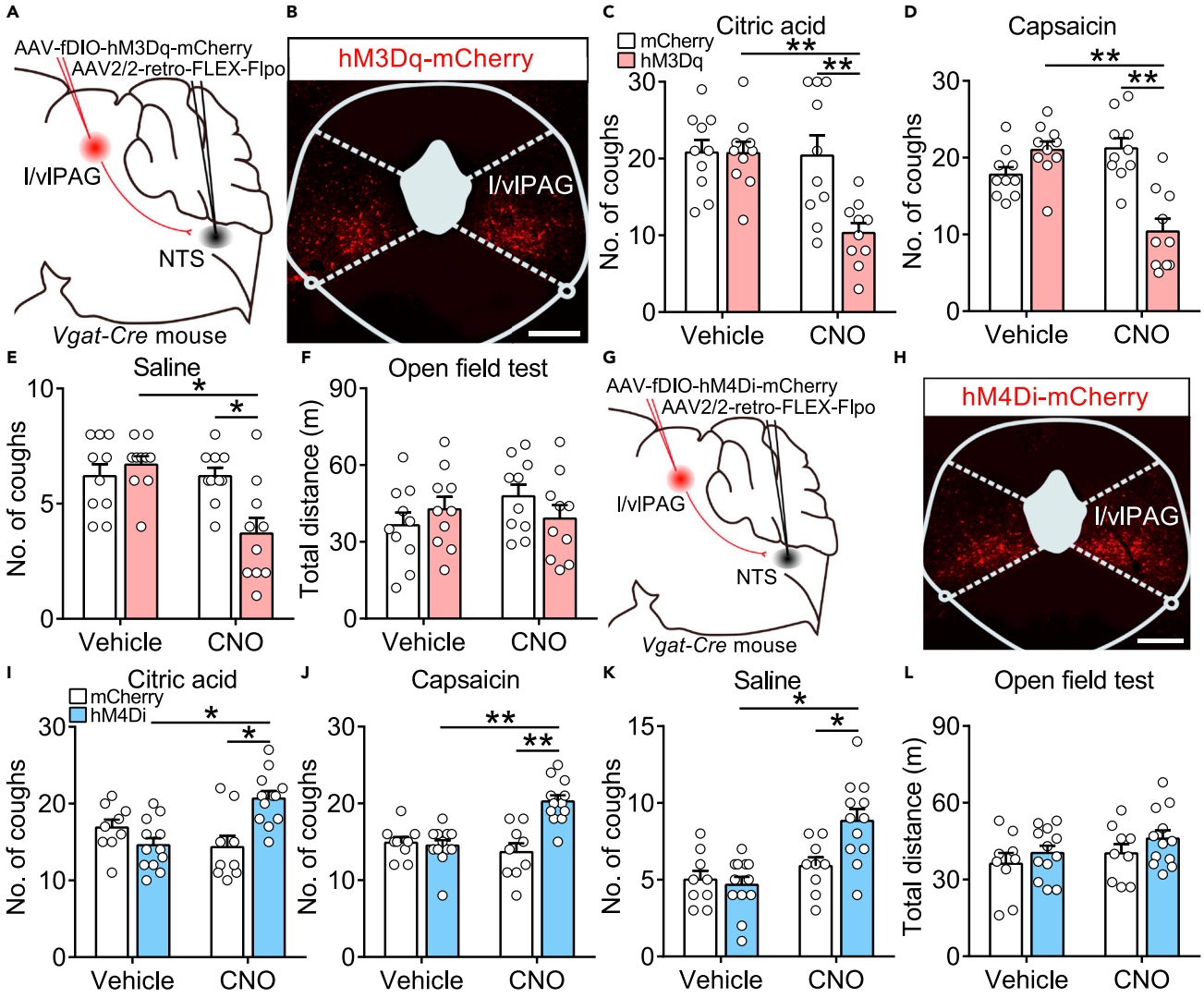

Figure 5. Pharmacogenetic manipulation of l/vlPAG GABAergic neurons projecting to the NTS modulates cough sensitivity

(A) A schematic diagram showing the sites of AAV2/2-retro-FLEX-Flpo injection into the bilateral NTS and AAV-fDIO-hM3Dq-mCherry or AAV-fDIO-mGFP injection into the bilateral l/vlPAG of Vgat-Cre mice.

(B) Expression of hM3Dq-mCherry in the l/vlPAG. Scale bar, 300 μm.

(C–E) Effects of pharmacogenetic activation of l/vlPAG GABAergic neurons projecting to the NTS by injection of CNO (1 mg/kg, i.p.) on coughing-like behaviors induced by nebulized CA (C), capsaicin (D), or saline (E); two-way ANOVA (n = 10 mice).

(F) Effects of pharmacogenetic activation of l/vlPAG GABAergic neurons projecting to the NTS by injection of CNO (1 mg/kg, i.p.) on locomotion; two-way ANOVA (n = 10 mice).

(G) A schematic diagram showing the sites of AAV2/2-retro-FLEX-Flpo injection into the bilateral NTS and AAV-fDIO-hM4Di-mCherry or AAV-fDIO-mGFP injection into the bilateral l/vlPAG of Vgat-Cre mice.

(H) Expression of hM4Di-mCherry in the l/vlPAG. Scale bar, 300 μm.

(I–K) Effects of pharmacogenetic inhibition of l/vlPAG GABAergic neurons projecting to the NTS by injection of CNO (1 mg/kg, i.p.) on coughing-like behaviors induced by nebulized CA (I), capsaicin (J), or saline (K); two-way ANOVA (n = 9 or 12 mice).

(L) Effects of pharmacogenetic inhibition of l/vlPAG GABAergic neurons projecting to the NTS by injection of CNO (1 mg/kg, i.p.) on locomotion; two-way ANOVA (n = 9 or 12 mice). All error bars represent the SEMs. *p <0.05, **p <0.01.

were slightly different from those monitored by our system. This may be due to different mouse strains, as they monitored coughing-like responses of BALB/c mice. Using a similar monitoring system, a recent study reported that capsaicin could also trigger sneezes in mice (Li et al., 2021). The box flows of sneeze are more sharply without an inspiration phase. Besides, the number of sneezes (~60 times in 5 min) triggered by nebulized capsaicin (~10 μm) is much larger than that of coughs (~15 times in 10 min). To further confirm that our monitored

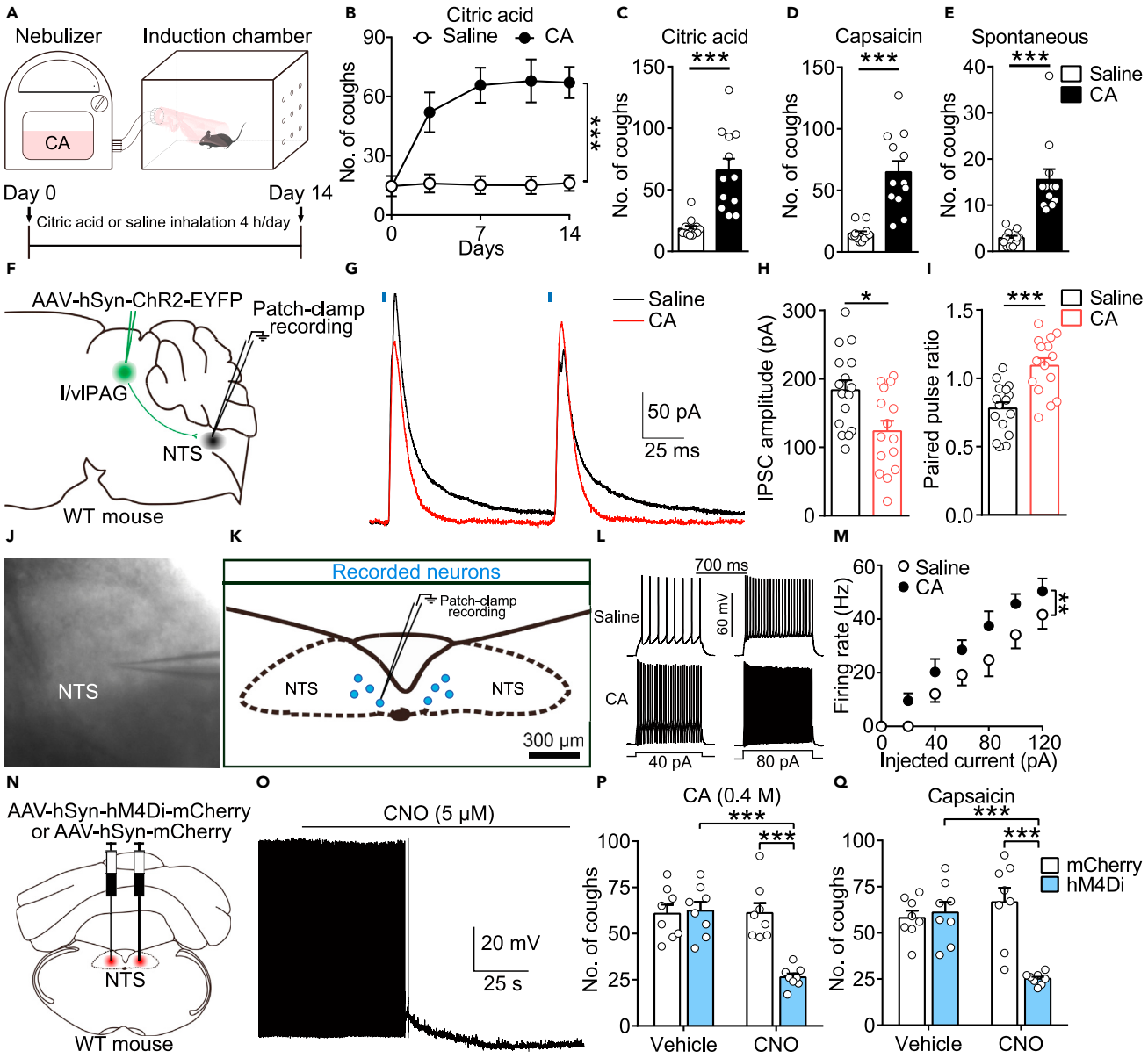

Figure 6. Decreased l/vlPAG GABAergic inputs to the NTS in mice with chronic cough

(A) A schematic diagram showing repeated airway stimulation by nebulized CA or saline and a timeline of the behavioral experiments.

(B) Time course of saline or CA exposure-induced coughing-like behavior; two-way ANOVA (n = 12 mice).

(C–E) The effects of 14 days of saline or CA inhalation on coughing-like behavior induced by nebulized CA (C), capsaicin (D), or saline (E); Mann-Whitney test (n = 12 mice).

(F) A schematic diagram showing the sites of AAV-hSyn-ChR2-EYFP injection into the l/vlPAG of WT mice and patch-clamp recording of NTS neurons.

(G) Representative optically evoked IPSCs recorded in NTS neurons of mice treated with CA or saline. Blue bar, LED stimulation (475 nm, 1 ms).

(H) The IPSCs of mice treated with CA were smaller than those of mice treated with saline (n = 16 neurons from 6 mice treated with saline, n = 15 neurons from 5 mice treated with CA); Mann-Whitney test.

(I) The PPRs (P2/P1) of l/vlPAG GABAergic inputs to NTS neurons in mice treated with CA were significantly larger than those in mice treated with saline (n = 16 neurons from 6 mice treated with saline, n = 15 neurons from 5 mice treated with CA); Mann-Whitney test.

(J) A representative image of the position of a recorded NTS neuron in a WT mouse.

(K) A schematic showing the experimental configuration for recordings in brain slices from WT mice.

(L and M) Sample traces of and statistical data for action potentials recorded from NTS neurons in mice treated with saline or CA inhalation (n = 12 neurons from 5 mice treated with saline, n = 14 neurons from 5 mice treated with CA); two-way ANOVA.

(N) A schematic diagram showing the sites of AAV-hSyn-hM4Di-mCherry or AAV-hSyn-mCherry virus injection into the bilateral NTS of WT mice.

(O) Effect of bath application of CNO on spikes of a representative hM4Di-mCherry^{+} NTS neuron.

(P and Q) The effects of the inhibition of NTS neurons on coughing-like behavior induced by CA (P) or capsaicin (Q); two-way ANOVA (n = 8 mice). All error bars represent the SEMs. *p <0.05, **p <0.01, ***p <0.001.

coughing-like responses were coughs but not sneeze, we transected the cervical nerve or the AEN of mice, as cough reflexes are selectively mediated by the cervical nerve and sneezing reflexes are specifically mediated by the AEN (Batsel and Lines, 1978; Li et al., 2021; Polverino et al., 2012). After UCV, the monitored CA- or capsaicin-evoked coughing-like behaviors is largely abolished. In contrast, AEN transection did not have any impact on the number of monitored coughing-like behaviors. Thus, we successfully established a mouse model for monitoring cough reflexes.

The l/vlPAG contributes to multiple sensations

The l/vlPAG neurons play important roles in modulating respiration and somatosensory processing (Faull et al., 2019; Gao et al., 2019; Samineni et al., 2017, 2019). Our results demonstrated that the activity of l/vlPAG neurons was elevated during tussive agent-induced coughing-like behaviors, which is consistent with previous studies showing that the l/vlPAG of patients with chronic cough is activated by inhalation of capsaicin (Ando et al., 2016). Global excitation of l/vlPAG neurons in turn suppressed cough signal processing, which is consistent with previous studies showing that electric stimulation of periaqueductal gray suppresses coughing-like behaviors (Sessle et al., 1981). This notion was supported by experiments showing that pharmacogenetic activation of these l/vlPAG neurons alleviated coughing-like behaviors evoked by tussive agents. In contrast, global inhibition of l/vlPAG neurons facilitated coughing-like behaviors, leading to cough hypersensitivity.

There is a large number of neuronal subtypes in the l/vlPAG, including GABAergic, glutamatergic, tachykinin 1-positive, and somatostatin-positive neurons (Gao et al., 2019; Samineni et al., 2017). Among these neuronal subtypes, GABAergic neurons have been shown to be important for regulating itch and pain processing (Samineni et al., 2017, 2019). Therefore, we examined the potential role of l/vlPAG GABAergic neurons in modulating cough sensitivity. We found that l/vlPAG GABAergic neurons play a key role in gating cough processing, as evidenced by the behavioral results showing that activation of l/vlPAG GABAergic neurons inhibited tussive agent-evoked coughing-like behaviors. Consistently, inhibition of l/vlPAG GABAergic neurons amplified the cough signal, leading to a large number of coughs induced by the nonirritant saline. This is in line with the gating effect of l/vlPAG GABAergic neurons in itch processing but opposite that in pain processing (Samineni et al., 2017, 2019). There may be several reasons for this phenomenon. There are numerous physiological, anatomic, pathogenic, and mechanistic similarities between cough and itch (Lavinka and Dong, 2013; Pecova et al., 2020). In addition, pain is well known for its antipruritic effect (Ikoma et al., 2003; Koch et al., 2018). Pain induced by noxious cold can also suppress the coughing-like behaviors evoked by capsaicin (Hilton et al., 2020). Thus, the central neural pathways that regulate pain processing might have functions that are opposite of those that control itch and cough processing. However, how the higher brains modulate coughing-like behaviors through regulating the activity of l/vlPAG GABAergic neurons remains to be further examined.

The l/vlPAG receives inputs from multiple sensory-related regions, including the prefrontal cortex, amygdala, parabrachial nucleus, and spinal cord; thus, the l/vlPAG might be critical in integrating both somatosensation and airway sensation. Therefore, the l/vlPAG might serve as a hub for the integration of multiple sensory information and regulated the interaction between different kinds of sensations.

The l/vlPAG-NTS inhibitory pathway modulates cough sensitivity

Cough signals are initiated in the airways and lungs and are transmitted to the central nervous system via two ascending pathways (Mazzone and Undem, 2016). One is specific for nodose ganglia-derived afferent fibers projecting to the NTS; the other is specific for jugular ganglia-derived afferent fibers projecting to the paratrigeminal nucleus (Pa5) (Mazzone and Undem, 2016; McGovern et al., 2017; Singh et al., 2020). In addition, the NTS is a downstream target of the l/vlPAG (Farkas et al., 1997; Gasparini et al., 2020) and thus considered to be involved in the descending regulation of cough sensitivity, at least for the nodose ganglia-derived ascending pathway (Mazzone et al., 2015; McGovern et al., 2017).

Our findings suggested that l/vlPAG neurons form inhibitory synapses with NTS neurons. The existence of direct synaptic connections between l/vlPAG and NTS neurons was further supported by the retrograde tracing results. Given that the NTS transmits vagal sensory information from the airway and lungs and plays an important role in regulating cough sensitivity (Cinelli et al., 2016; Gestreau et al., 1997; Haji et al., 2012; Jakus et al., 2008; Mutolo et al., 2007, 2008), l/vlPAG GABAergic projections may directly suppress cough processing via the NTS. Therefore, dysfunction of this l/vlPAG-NTS GABAergic projection could result in cough hypersensitivity. This is supported by the following four pieces of evidence. First, selective suppression of NTS-projecting l/vlPAG

GABAergic neurons promoted coughing-like reflex behaviors. Second, selective activation of l/vlPAG GABAergic neurons projecting to the NTS impaired cough processing. These two results also exclude the possibility that the effect of l/vlPAG GABAergic neuron manipulation on coughing-like behaviors was due to direct control of the motor pathway, highlighting the important role of l/vlPAG GABAergic neurons in modulating sensory processing of cough. Third, inhibitory synapses between the l/vlPAG and the NTS were weaker in cough hypersensitivity model mice. Finally, inhibition of NTS neurons alleviated cough hypersensitivity in cough hypersensitivity model mice. We also examined the potential role of l/vlPAG glutamatergic neurons in addition to GABAergic neurons. We found that l/vlPAG glutamatergic neurons projecting to the NTS play an insignificant role in modulating cough sensitivity, as evidenced by the fact that manipulation of l/vlPAG glutamatergic neurons projecting to the NTS did not significantly affect nonirritant saline and tussive agent-evoked coughing-like behaviors. Consistently, we showed that the probability of l/vlPAG glutamatergic neurons forming synapses with NTS neurons is very low and that there are few l/vlPAG glutamatergic neurons projecting to the NTS. Although we emphasized the essential role of l/vlPAG GABAergic neuron-mediated regulation of NTS neuron activity, we did not exclude the possibility that other l/vlPAG subpopulations might also play a role in regulating the cough pathways and that l/vlPAG GABAergic neurons could also influence cough sensitivity through other brain regions. It has been shown that l/vlPAG neurons can also send projection axons to the rostral ventromedial medulla, Pa5, and other related areas involved in cough processing (McGovern et al., 2017; Sessle et al., 1981).

In summary, we have identified an important pathway for the descending regulation of cough sensitivity. Our study provides a cellular and circuit basis for push-pull regulation of cough, whereby dysfunction of the descending modulatory pathway may induce disinhibition of the cough pathway, leading to cough hypersensitivity. The top-down pathway might be recruited during the development of cough hypersensitivity and may thus be a potential central therapeutic target for the treatment of refractory cough and unexplained chronic cough.

Limitations of the study

This study has not determined the role of other downstream brain regions of l/vlPAG GABAergic neurons in regulating cough sensitivity and mediating cough hypersensitivity. In addition, it is unknown how the l/vlPAG GABAergic neurons are regulated by higher brain areas in cough hypersensitivity model mice. Furthermore, our AAV-based retrograde strategy cannot label all NTS-projecting l/vlPAG GABAergic neurons. The unlabeled GABAergic neurons and other subpopulations of l/vlPAG neurons might also project to the NTS and regulate cough sensitivity. Future studies will be required to fully dissect the functional role of descending pathways in modulating cough sensitivity via the l/vlPAG.

STAR★METHODS

Detailed methods are provided in the online version of this paper and include the following:

- KEY RESOURCES TABLE
- RESOURCE AVAILABILITY
  - Lead contact
  - Materials availability
  - Data and code availability
- EXPERIMENTAL MODEL AND SUBJECT DETAILS
- METHOD DETAILS
  - Detection of cough-like behaviors in mice
  - Animal model of cough hypersensitivity
  - Open field test
  - Surgery for viral injection into the brain
  - Pharmacogenetic manipulations
  - Immunofluorescent staining
  - Electrophysiological slice recording
- QUANTIFICATION AND STATISTICAL ANALYSIS

SUPPLEMENTAL INFORMATION

Supplemental information can be found online at https://doi.org/10.1016/j.isci.2021.103641.

ACKNOWLEDGMENTS

We thank Xin Liu and Su-Bo Zhang for their technical support. This work is supported by the National Natural Science Foundation of China (No. 82100120, 81770098, 31900717, and 81900100), Guangdong-Hong Kong-Macao Joint Laboratory of Respiratory Infectious Disease (No. 02-000-2101-5079), and Zhongnanshan Medical Foundation of Guangdong Province (No. ZNSA-2020013).

AUTHOR CONTRIBUTIONS

Z.C., D.M., and M.J.L. performed the electrophysiology experiments and analyzed the data. M.-T.L. performed the virus injection and immunofluorescent staining experiment. Z.C., M.-T.L., C.Z., and M.J.L. performed the behavioral experiments. N.-S.Z., D.M., K.-F.L., and M.J.L. designed the experiments and wrote the manuscript.

DECLARATION OF INTERESTS

The authors declare no competing interests.

Received: September 15, 2021
Revised: November 11, 2021
Accepted: December 13, 2021
Published: January 21, 2022

REFERENCES

Ando, A., Smallwood, D., McMahon, M., Irving, L., Mazzone, S.B., and Farrell, M.J. (2016). Neural correlates of cough hypersensitivity in humans: evidence for central sensitisation and dysfunctional inhibitory control. Thorax *71*, 323–329.

Armbruster, B.N., Li, X., Pausch, M.H., Herlitze, S., and Roth, B.L. (2007). Evolving the lock to fit the key to create a family of G protein-coupled receptors potently activated by an inert ligand. Proc. Natl. Acad. Sci. U S A *104*, 5163–5168.

Batsel, H.L., and Lines, A.J. (1978). Discharge of respiratory neurons in sneezes resulting from ethmoidal nerve stimulation. Exp. Neurol. *58*, 410–424.

Bautista, T.G., Leech, J., Mazzone, S.B., and Farrell, M.J. (2019). Regional brain stem activations during capsaicin inhalation using functional magnetic resonance imaging in humans. J. Neurophysiol. *121*, 1171–1182.

Bolser, D.C. (2004). Experimental models and mechanisms of enhanced coughing. Pulm. Pharmacol. Ther. *17*, 383–388.

Chen, L., Lai, K., Lomask, J.M., Jiang, B., and Zhong, N. (2013). Detection of mouse cough based on sound monitoring and respiratory airflow waveforms. PLoS One *8*, e59263.

Chen, Z., Gu, D., Fan, L., Zhang, W., Sun, L., Chen, H., Dong, R., and Lai, K. (2019). Neuronal activity of the medulla oblongata revealed by manganese-enhanced magnetic resonance imaging in a rat model of gastroesophageal reflux-related cough. Physiol. Res. *68*, 119–127.

Cinelli, E., Iovino, L., Bongianni, F., Pantaleo, T., and Mutolo, D. (2016). GABAA- and glycine-mediated inhibitory modulation of the cough reflex in the caudal nucleus tractus solitarii of the rabbit. Am. J. Physiol. Lung Cell Mol. Physiol. *311*, L570–L580.

Driessen, A.K., McGovern, A.E., Behrens, R., Moe, A.A.K., Farrell, M.J., and Mazzone, S.B. (2020). A role for neurokinin 1 receptor expressing neurons in the paratrigeminal nucleus in bradykinin-evoked cough in guinea-pigs. J. Physiol. *598*, 2257–2275.

Everett, C.F., Kastelik, J.A., Thompson, R.H., and Morice, A.H. (2007). Chronic persistent cough in the community: a questionnaire survey. Cough *3*, 5.

Farkas, E., Jansen, A.S., and Loewy, A.D. (1997). Periaqueductal gray matter projection to vagal preganglionic neurons and the nucleus tractus solitarius. Brain Res. *764*, 257–261.

Faull, O.K., Subramanian, H.H., Ezra, M., and Pattinson, K.T.S. (2019). The midbrain periaqueductal gray as an integrative and interoceptive neural structure for breathing. Neurosci. Biobehav Rev. *98*, 135–144.

Gao, Z.R., Chen, W.Z., Liu, M.Z., Chen, X.J., Wan, L., Zhang, X.Y., Yuan, L., Lin, J.K., Wang, M., Zhou, L., et al. (2019). Tac1-Expressing neurons in the periaqueductal gray facilitate the itch-scratching cycle via descending regulation. Neuron *101*, 45–59 e49.

Gasparini, S., Howland, J.M., Thatcher, A.J., and Geerling, J.C. (2020). Central afferents to the nucleus of the solitary tract in rats and mice. J. Comp. Neurol. *528*, 2708–2728.

Gestreau, C., Bianchi, A.L., and Grelot, L. (1997). Differential brainstem Fos-like immunoreactivity after laryngeal-induced coughing and its reduction by codeine. J. Neurosci. *17*, 9340–9352.

Haji, A., Ohi, Y., and Kimura, S. (2012). Cough-related neurons in the nucleus tractus solitarius of decerebrate cats. Neuroscience *218*, 100–109.

Hilton, E., Satia, I., Holt, K., Woodcock, A.A., Belcher, J., and Smith, J.A. (2020). The effect of pain conditioning on experimentally evoked cough: evidence of impaired endogenous inhibitory control mechanisms in refractory chronic cough. Eur. Respir. J. *56*, 2001387.

Ikoma, A., Rukwied, R., Stander, S., Steinhoff, M., Miyachi, Y., and Schmelz, M. (2003). Neurophysiology of pruritus: interaction of itch and pain. Arch. Dermatol. *139*, 1475–1478.

Jakus, J., Poliacek, I., Halasova, E., Murin, P., Knocikova, J., Tomori, Z., and Bolser, D.C. (2008). Brainstem circuitry of tracheal-bronchial cough: c-fos study in anesthetized cats. Respir. Physiol. Neurobiol. *160*, 289–300.

Koch, S.C., Acton, D., and Goulding, M. (2018). Spinal circuits for touch, pain, and itch. Annu. Rev. Physiol. *80*, 189–217.

Lavinka, P.C., and Dong, X. (2013). Molecular signaling and targets from itch: lessons for cough. Cough *9*, 8.

Li, F., Jiang, H., Shen, X., Yang, W., Guo, C., Wang, Z., Xiao, M., Cui, L., Luo, W., Kim, B.S., et al. (2021). Sneezing reflex is mediated by a peptidergic pathway from nose to brainstem. Cell *184*, 3762–3773 e3710.

Li, Y., Zeng, J., Zhang, J., Yue, C., Zhong, W., Liu, Z., Feng, Q., and Luo, M. (2018). Hypothalamic circuits for predation and evasion. Neuron *97*, 911–924 e915.

Lin, R.L., Gu, Q., Khosravi, M., and Lee, L.Y. (2017). Sustained sensitizing effects of tumor necrosis factor alpha on sensory nerves in lung and airways. Pulm. Pharmacol. Ther. *47*, 29–37.

Liu, M.Z., Chen, X.J., Liang, T.Y., Li, Q., Wang, M., Zhang, X.Y., Li, Y.Z., Sun, Q., and Sun, Y.G. (2019). Synaptic control of spinal GRPR(+) neurons by local and long-range inhibitory inputs. Proc. Natl. Acad. Sci. U S A *116*, 27011–27017.

Mazzone, S.B., McGovern, A.E., and Farrell, M.J. (2015). Endogenous central suppressive

mechanisms regulating cough as potential targets for novel antitussive therapies. Curr. Opin. Pharmacol. *22*, 1–8.

Mazzone, S.B., and Undem, B.J. (2016). Vagal afferent innervation of the airways in health and disease. Physiol. Rev. *96*, 975–1024.

McGovern, A.E., Ajayi, I.E., Farrell, M.J., and Mazzone, S.B. (2017). A neuroanatomical framework for the central modulation of respiratory sensory processing and cough by the periaqueductal grey. J. Thorac. Dis. *9*, 4098–4107.

McGovern, A.E., Davis-Poynter, N., Yang, S.K., Simmons, D.G., Farrell, M.J., and Mazzone, S.B. (2015a). Evidence for multiple sensory circuits in the brain arising from the respiratory system: an anterograde viral tract tracing study in rodents. Brain Struct. Funct. *220*, 3683–3699.

McGovern, A.E., Driessen, A.K., Simmons, D.G., Powell, J., Davis-Poynter, N., Farrell, M.J., and Mazzone, S.B. (2015b). Distinct brainstem and forebrain circuits receiving tracheal sensory neuron inputs revealed using a novel conditional anterograde transsynaptic viral tracing system. J. Neurosci. *35*, 7041–7055.

Morice, A.H., Fontana, G.A., Belvisi, M.G., Birring, S.S., Chung, K.F., Dicpinigaitis, P.V., Kastelik, J.A., McGarvey, L.P., Smith, J.A., Tatar, M., et al. (2007). ERS guidelines on the assessment of cough. Eur. Respir. J. *29*, 1256–1276.

Morice, A.H., Millqvist, E., Belvisi, M.G., Bieksiene, K., Birring, S.S., Chung, K.F., Dal Negro, R.W., Dicpinigaitis, P., Kantar, A., McGarvey, L.P., et al. (2014). Expert opinion on the cough hypersensitivity syndrome in respiratory medicine. Eur. Respir. J. *44*, 1132–1148.

Morice, A.H., Millqvist, E., Bieksiene, K., Birring, S.S., Dicpinigaitis, P., Ribas, C.D., Boon, M.H., Kantar, A., Lai, K., McGarvey, L., et al. (2019). ERS guidelines on the diagnosis and treatment of chronic cough in adults and children. Eur. Respir. J. *55*, 1901136.

Mutolo, D., Bongianni, F., Cinelli, E., Fontana, G.A., and Pantaleo, T. (2008). Modulation of the cough reflex by antitussive agents within the caudal aspect of the nucleus tractus solitarii in the rabbit. Am. J. Physiol. Regul. Integr. Comp. Physiol. *295*, R243–R251.

Mutolo, D., Bongianni, F., Fontana, G.A., and Pantaleo, T. (2007). The role of excitatory amino acids and substance P in the mediation of the cough reflex within the nucleus tractus solitarii of the rabbit. Brain Res. Bull. *74*, 284–293.

Nakaji, H., Niimi, A., Matsuoka, H., Iwata, T., Cui, S., Matsumoto, H., Ito, I., Oguma, T., Otsuka, K., Takeda, T., et al. (2016). Airway remodeling associated with cough hypersensitivity as a consequence of persistent cough: an experimental study. Respir. Invest. *54*, 419–427.

Nectow, A.R., and Nestler, E.J. (2020). Viral tools for neuroscience. Nat. Rev. Neurosci. *21*, 669–681.

Ovsyannikov, E.S., Avdeev, S.N., Budnevsky, A.V., and Shkatova, Y.S. (2019). Influence of anxiety/depression on the subjective evaluation of cough in patients with chronic obstructive pulmonary disease and obesity. Medicina (Kaunas) *55*, 134.

Pecova, T., Kocan, I., Vysehradsky, R., and Pecova, R. (2020). Itch and cough - similar role of sensory nerves in their pathogenesis. Physiol. Res. *69*, S43–S54.

Polverino, M., Polverino, F., Fasolino, M., Ando, F., Alfieri, A., and De Blasio, F. (2012). Anatomy and neuro-pathophysiology of the cough reflex arc. Multidiscip Respir. Med. *7*, 5.

Ruhl, C.R., Pasko, B.L., Khan, H.S., Kindt, L.M., Stamm, C.E., Franco, L.H., Hsia, C.C., Zhou, M., Davis, C.R., Qin, T., et al. (2020). *Mycobacterium tuberculosis* sulfolipid-1 activates nociceptive neurons and induces cough. Cell *181*, 293–305 e211.

Samineni, V.K., Grajales-Reyes, J.G., Copits, B.A., O'Brien, D.E., Trigg, S.L., Gomez, A.M., Bruchas, M.R., and Gereau, R.W.t. (2017). Divergent modulation of nociception by glutamatergic and GABAergic neuronal subpopulations in the periaqueductal gray. eNeuro *4*, 0116–0129.

Samineni, V.K., Grajales-Reyes, J.G., Sundaram, S.S., Yoo, J.J., and Gereau, R.W.t. (2019). Cell type-specific modulation of sensory and affective components of itch in the periaqueductal gray. Nat. Commun. *10*, 4356.

Sessle, B.J., Ball, G.J., and Lucier, G.E. (1981). Suppressive influences from periaqueductal gray and nucleus raphe magnus on respiration and related reflex activities and on solitary tract neurons, and effect of naloxone. Brain Res. *216*, 145–161.

Silver, R.A., Momiyama, A., and Cull-Candy, S.G. (1998). Locus of frequency-dependent depression identified with multiple-probability fluctuation analysis at rat climbing fibre-Purkinje cell synapses. J. Physiol. *510*, 881–902.

Singh, N., Driessen, A.K., McGovern, A.E., Moe, A.A.K., Farrell, M.J., and Mazzone, S.B. (2020). Peripheral and central mechanisms of cough hypersensitivity. J. Thorac. Dis. *12*, 5179–5193.

Tervo, D.G., Hwang, B.Y., Viswanathan, S., Gaj, T., Lavzin, M., Ritola, K.D., Lindo, S., Michael, S., Kuleshova, E., Ojala, D., et al. (2016). A designer AAV variant permits efficient retrograde Access to projection neurons. Neuron *92*, 372–382.

Urban, D.J., and Roth, B.L. (2015a). DREADDs (designer receptors exclusively activated by designer drugs): chemogenetic tools with therapeutic utility. Annu. Rev. Pharmacol. Toxicol. *55*, 399–417.

Urban, D.J., and Roth, B.L. (2015b). DREADDs (designer receptors exclusively activated by designer drugs): chemogenetic tools with therapeutic utility. Annu. Rev. Pharmacol. Toxicol. *55*, 399–417.

Yu, L., Tsuji, K., Ujihara, I., Liu, Q., Pavelkova, N., Tsujimura, T., Inoue, M., Meeker, S., Nisenbaum, E., McDermott, J.S., et al. (2021). Antitussive effects of NaV 1.7 blockade in Guinea pigs. Eur. J. Pharmacol. *907*, 174192.

Zhang, C., Lin, R.L., Hong, J., Khosravi, M., and Lee, L.Y. (2017). Cough and expiration reflexes elicited by inhaled irritant gases are intensified in ovalbumin-sensitized mice. Am. J. Physiol. Regul. Integr. Comp. Physiol. *312*, R718–R726.

STAR★METHODS

KEY RESOURCES TABLE

REAGENT or RESOURCE	SOURCE	IDENTIFIER
Antibodies		
Rabbit anti-GFP	Thermo Fisher Scientific	Cat#A-11122; RRID: AB_221569
Rabbit anti-DsRed	Clontech	Cat#632496; RRID: AB_10013483
Rabbit anti-c-Fos	Synaptic System	Cat#226003; RRID: AB_2231974
Donkey anti-rabbit IgG-Alexa 488	Jackson ImmunoResearch Laboratories	Cat#711-545-152; RRID: AB_2313584
Donkey anti-rabbit IgG-Cy3	Jackson ImmunoResearch Laboratories	Cat#711-165-152; RRID: AB_2307443
Bacterial and virus strains		
AAV2/8-hSyn-hM3Dq-mCherry	Shanghai Taitool Bioscience	Cat#S0425-8
AAV2/8-hSyn-hM4Di-mCherry	Shanghai Taitool Bioscience	Cat#S0279-8
AAV2/8-hSyn-mCherry	Shanghai Taitool Bioscience	Cat#S0238-8
AAV2/5-hSyn-DIO-hM3Dq-mCherry	Shanghai Taitool Bioscience	Cat#S0192-5
AAV2/5-hSyn-DIO-hM4Di-mCherry	Shanghai Taitool Bioscience	Cat#S0193-5
AAV2/5-hSyn-DIO-mCherry	Shanghai Taitool Bioscience	Cat#S0240-5
AAV2/9-hSyn-EGFP	Shanghai Taitool Bioscience	Cat#S0237-9
AAV2/2-retro-hSyn-Cre	Shanghai Taitool Bioscience	Cat#S0278-2R
AAV2/9-hSyn-hChR2(H134R)-EYFP	Shanghai Taitool Bioscience	Cat#S0318-9
AAV2/2-retro-FLEX-Flpo	Shanghai Taitool Bioscience	Cat#S0273-2R
AAV2/9-fDIO-hM3Dq-mCherry	Shanghai Taitool Bioscience	Cat#S0337-9
AAV2/9-fDIO-hM4Di-mCherry	Shanghai Taitool Bioscience	Cat#S0336-9
AAV2/5-fDIO-mGFP	Shanghai Taitool Bioscience	Cat#S0289-5
Chemicals, peptides, and recombinant proteins		
Clozapine-n-oxide	Sigma-Aldrich	Cat#C0832
NBQX	Tocris	Cat#1044
Picrotoxin	Tocris	Cat#1128
Citric acid	Sigma-Aldrich	Cat#C2404
Capsaicin	Sigma-Aldrich	Cat#M2028
Experimental models: Organisms/strains		
Mouse: C57BL/6N	Guangdong Medical Laboratory Animal Center or Gene & Peace Co., Ltd. (Guangdong)	N/A
Mouse: Vgat-ires-Cre	The Jackson Laboratory	JAX: 016962
Mouse: Vglut2-Cre	The Jackson Laboratory	JAX: 016963
Mouse: Ai9	The Jackson Laboratory	JAX: 007909
Software and algorithms		
GraphPad Prism 5	GraphPad	https://www.graphpad.com/scientificsoftware/prism/
Fiji (ImageJ)	NIH	https://fiji.sc/
Photoshop CS6	Adobe	https://www.adobe.com/
Illustrator CS6	Adobe	https://www.adobe.com/
Clampfit 10.3	Molecular Devices	https://www.moleculardevices.com.cn/

RESOURCE AVAILABILITY

Lead contact

Further information and requests for resources and reagents should be directed to and will be fulfilled by the lead contact, Mingzhe J. Liu (lmzrondo@ustc.edu).

Materials availability

This study did not generate new unique reagents.

Data and code availability

All relevant datasets and analysis are included in this article and in the supplemental information, or are available from the lead contact upon reasonable request.

All original code is available from the lead contact upon reasonable request.

Any additional information required to reanalyze the data reported in this work paper is available from the lead contact upon request.

EXPERIMENTAL MODEL AND SUBJECT DETAILS

Male *C57BL/6N*, *Vgat-ires-Cre*, *Vglut2-Cre* and *Ai9* mice were used for the experiments. *C57BL/6N* mice were purchased from Guangdong Medical Laboratory Animal Center or Gene & Peace Co., Ltd. (Guangdong). *Vgat-ires-Cre* (JAX016962), *Vglut2-Cre* (JAX016963) and *Ai9* (JAX007909) mice were initially acquired from Jackson Laboratory. All procedures were approved by the Animal Care and Use Committee of the State Key Laboratory of Respiratory Disease, The First Affiliated Hospital of Guangzhou Medical University, Guangzhou, China. All mice were housed on a 12-hr light/dark cycle (lights on at 7:00 am) with *ad libitum* access to food and water. For behavioral tests and electrophysiological recordings, all animals were between 8-14 weeks old at the time of experiments. The animals were randomly allocated to different groups where appropriate. All behavioral tests were carried out during the light phase. Researchers were blinded to mouse genotypes and treatment for behavioral tests and data analysis.

METHOD DETAILS

Detection of cough-like behaviors in mice

The coughing-like reflex was recorded in mice using the Buxco Small Animal Whole Body Plethysmography System (DSI, 601-1400-001 Rev13) and analyzed using FinePointe Software (DSI, 007898-001 Rev03). The mice were placed in a DSI noninvasive WBP chamber (DSI, 601-1425-001), and a mini microphone (Bailing, Shandong) was mounted onto the lateral aperture of the WBP chamber. The output port was connected to the computer, and sound waves were recorded with sound analysis software (Adobe Audition). The WBP chamber was connected to a signal converter, and airflow changes in the chamber were converted to respiratory waveforms with FinePointe cough detection software for recording and automated real-time analysis. Nebulized CA (Sigma, C2404; 0.1 or 0.4 M), capsaicin (Sigma, M2028; 0.01 mM) and normal saline were used for the cough challenge.

The experimental animals were habituated to the testing room for at least two days before the behavioral tests. The animals were placed in the recording chamber for 30 minutes for habituation. Coughing-like reflex behavior was recorded for 10 min. Coughing-like behaviors were identified from respiratory traces generated by FinePointe software and the WBP system. For video and audio recordings, a video camera (Canon, VIXIA HFG10) was placed on the top of the recording chamber. For simultaneous WBP and audio recordings, a mini audio recorder (aTTo digital, 16 kHz) was placed in the WBP recording chamber. Audio components were extracted from video files and analyzed using Audacity software.

For tussive agent-induced coughing-like behaviors, 1 mL of test solution was delivered over 10 min using a nebulizer (Aerogen Pro). Citric acid, capsaicin and saline inhalation challenges were performed in random order. In terms of the DREADD manipulation, it was always vehicle then CNO, as shown in the following flow diagram (Figure S7).

Animal model of cough hypersensitivity

Naive mice were exposed to CA (0.1 M) via a nebulizer for 4 h/day for 14 days. The control group were exposed to nebulized saline. The number of coughing-like behaviors induced by CA (0.4 M) was counted on day 0, day 3, day 7, day 11 and day 14. After 14-day CA or saline exposure, the cough sensitivity of mice was assessed by inhalation of nebulized CA (0.4 M), capsaicin (0.01 mM) or saline.

Open field test

The animals were habituated to the testing room for at least two days before the behavioral tests. The locomotor activity of mice was evaluated over a 10-min period in 40 × 40 × 40 cm polystyrene enclosures by the open field test. The mice were placed in the center of the box and videotaped individually. The traces were analyzed with LabState software (AniLab).

Surgery for viral injection into the brain

The mice were anesthetized with pentobarbital sodium (100 mg/kg; MYM Technologies Ltd.) and mounted in a stereotaxic apparatus (RWD Life Science Co., Ltd., 68513). The skull was exposed through a midline scalp incision, and unilateral or bilateral craniotomy was performed to introduce a glass microinjection pipette into the target brain regions. The craniotomy window (~1.5 mm in diameter) was made using a hand-held drill (RWD Life Science Co., Ltd.) over the target area.

To manipulate neurons in the l/vlPAG, AAV-hSyn-hM3Dq-mCherry (AAV2/8, titer: 4.7×10^{12} v.g./mL, Shanghai Taitool Bioscience Co. Ltd., S0425-8) or AAV-hSyn-hM4Di-mCherry (AAV2/8, titer: 4.3×10^{12} v.g./mL, Shanghai Taitool Bioscience Co. Ltd. S0279-8) was bilaterally injected into the l/vlPAG (anteroposterior (AP), −4.6 mm; mediolateral (ML), ±0.5 mm; dorsoventral (DV), −2.7 mm) of WT mice in a volume of 300 nL for each side. The same volume of AAV-hSyn-mCherry (AAV2/8, titer: 4.1×10^{12} v.g./mL, Shanghai Taitool Bioscience Co. Ltd., S0238-8) was used as a control.

To manipulate neurons in the NTS, AAV-hSyn-hM4Di-mCherry (AAV2/8, titer: 4.3×10^{12} v.g./mL, Shanghai Taitool Bioscience Co. Ltd., S0279-8) was bilaterally injected into the NTS (AP, −7.56 mm; ML, ±0.4 mm; DV, −5.1-5.3 mm) of WT mice in a volume of 100 nL for each side. The same volume of AAV-hSyn-mCherry (AAV2/8, titer: 4.1×10^{12} v.g./mL, Shanghai Taitool Bioscience Co. Ltd., S0238-8) was used as a control.

To manipulate GABAergic neurons in the l/vlPAG, AAV-hSyn-DIO-hM3Dq-mCherry (AAV2/5, titer: 5.0×10^{12} v.g./mL, Shanghai Taitool Bioscience Co. Ltd., S0192-5) or AAV-hSyn-DIO-hM4Di-mCherry (AAV2/5, titer: 4.7×10^{12} v.g./mL, Shanghai Taitool Bioscience Co. Ltd., S0193-5) was bilaterally injected into the l/vlPAG (AP, −4.6 mm; ML, ±0.5 mm; DV, −2.7 mm) of *Vgat-Cre* mice in a volume of 300 nL for each side. The same volume of AAV-hSyn-DIO-mCherry (AAV2/5, titer: 5.1×10^{12} v.g./mL, Shanghai Taitool Bioscience Co. Ltd., S0240-5) was used as a control.

For anterograde tracing of l/vlPAG-NTS projections, AAV-hSyn-EGFP (AAV2/9, titer: 4.7×10^{12} v.g./mL, Shanghai Taitool Bioscience Co. Ltd., S0237-9) was unilaterally injected into the l/vlPAG (AP, −4.6 mm; ML, ±0.5 mm; DV, −2.7 mm) of WT mice in a volume of 300 nL. These mice were perfused 5 weeks later.

For retrograde tracing of l/vlPAG-NTS projections, AAV2/2-retro-hSyn-Cre (AAV2/2-retro, titer: 1.0×10^{13} v.g./mL, Shanghai Taitool Bioscience Co. Ltd., S0278-2R) was unilaterally injected into the NTS (AP, −7.56 mm; ML, ±0.4 mm; DV, −5.1-5.3 mm) of *Ai9* mice in a volume of 150 nL. These mice were perfused 5 weeks later.

To examine the functional projections from l/vlPAG to RVM neurons, AAV2/9-hSyn-hChR2(H134R)-EYFP (AAV2/9, titer: 5.3×10^{12} v.g./mL, Shanghai Taitool Bioscience Co. Ltd., S0318-9) was unilaterally injected into the l/vlPAG of WT mice (7 weeks old). These mice were subjected to slice electrophysiology experiments 4 weeks later.

To selectively manipulate l/vlPAG GABAergic neurons projecting to the NTS, we used a retrograde AAV tracer (AAV2/2-retro) combined with a pharmacogenetic technique. AAV2/2-retro-FLEX-Flpo (AAV2/Retro, titer: 1.0×10^{13} v.g./mL, Shanghai Taitool Bioscience Co. Ltd., S0273-2R) was bilaterally injected into the NTS (AP, −7.56 mm; ML, ±0.4 mm; DV, −5.1-5.3 mm) of *Vgat-Cre* mice in a volume of 150 nL for each site , and AAV-fDIO-hM3Dq-mCherry (AAV2/9, titer: 4.7×10^{12} v.g./mL, Shanghai Taitool Bioscience Co.

Ltd., S0337-9) or AAV-fDIO-hM4Di-mCherry (AAV2/9, titer: 4.4 × 10^{12} v.g./mL v.g./mL, Shanghai Taitool Bioscience Co. Ltd., S0336-9) was bilaterally injected into the l/vlPAG (AP, −4.6 mm; ML, ±0.5 mm; DV, −2.7 mm) in a volume of 300 nL for each side. The same volume of AAV-fDIO-mGFP (AAV2/5, titer: 5.2 × 10^{12} v.g./mL, Shanghai Taitool Bioscience Co. Ltd., S0289-5) was used as a control.

To selectively manipulate l/vlPAG glutamatergic neurons projecting to the NTS, we used a retrograde AAV tracer combined with a pharmacogenetic technique. AAV2/2-retro-FLEX-Flpo (AAV2/2-retro, titer: 1.0 × 10^{13} v.g./mL, Shanghai Taitool Bioscience Co. Ltd., S0273-2R) was bilaterally injected into the NTS (AP, −7.56 mm; ML, ±0.4 mm; DV, −5.1-5.3 mm) of *Vglut2-Cre* mice in a volume of 150 nL for each site, and AAV-fDIO-hM3Dq-mCherry (AAV2/9, titer: 4.7 × 10^{12} v.g./mL, Shanghai Taitool Bioscience Co. Ltd., S0337-9) or AAV-fDIO-hM4Di-mCherry (AAV2/9, titer: 4.4 × 10^{12} v.g./mL v.g./mL, Shanghai Taitool Bioscience Co. Ltd., S0336-9) was bilaterally injected into the l/vlPAG (AP, −4.6 mm; ML, ±0.5 mm; DV, −2.7 mm) in a volume of 300 nL for each side. The same volume of AAV-fDIO-mGFP (AAV2/5, titer: 5.2 × 10^{12} v.g./mL, Shanghai Taitool Bioscience Co. Ltd., S0289-5) was used as a control.

The viral vectors were injected into the target regions using calibrated glass microelectrodes connected to an infusion pump (Drummond, Nanoject III) at a rate of 20-30 nL/min. The micropipette was withdrawn 10 min later. For behavioral experiments, animals were allowed to recover for 3-5 weeks. The mice were then handled and habituated to the behavioral environment every day for one week before the behavioral tests. For all experiments, animals in which the injection sites were incorrect were excluded from further analysis.

Pharmacogenetic manipulations

For *in vivo* pharmacogenetic activation experiments, mice were injected with CNO (Sigma, C0832; 1 mg/kg, i.p.), and tussive agent-induced coughing-like reflex behavior was tested 30-40 min after CNO application.

Immunofluorescent staining

Mice were anesthetized with an overdose of pentobarbital sodium (100 mg/kg; MYM Technologies Ltd.), and perfused transcardially with phosphate-buffered saline (PBS, HyClone) followed by PBS containing 4% paraformaldehyde (PFA, Sigma). The brains were dissected, postfixed overnight at 4°C in 4% PFA, and cryoprotected in 30% sucrose in PBS at 4°C. Free-floating sections (40 μm) prepared with a cryostat (Leica CM 1950) were used for immunohistochemical staining. The tissues sections were blocked for 30 min at room temperature in PBST (0.3% Triton X-100) containing 5% normal donkey serum (NDS, Abcam) and then incubated with primary antibodies at 4°C overnight and secondary antibodies at room temperature for 2-3 h. The primary antibodies used for immunohistochemistry (IHC) were rabbit anti-GFP (1:1000, Thermo Fisher Scientific), rabbit anti-DsRed (1:1000, Clontech), and rabbit anti-c-Fos (1:2000, Synaptic System). The secondary antibodies that were used were donkey Alexa 488-conjugated anti-rabbit IgG (1:500, Jackson ImmunoResearch Laboratories) and Cy3-conjugated donkey anti-rabbit IgG (1:500, Jackson ImmunoResearch Laboratories). Images were taken using a Nikon Eclipse Ni-E fluorescence microscope. Cell counting was carried out manually or automatically using Fiji (NIH).

Electrophysiological slice recording

Eight to 12-week-old mice were deeply anesthetized by an overdose of pentobarbital sodium. The brains were extracted, and coronal brain slices (220 μm) were generated at a slicing speed of 0.12 mm/s in ice-cold cutting solution containing (in mM) sucrose 50, KCl 1.8, NaCl 95, KH_2PO_4 1.2, $MgSO_4$ 7, $CaCl_2$ 0.5, $NaHCO_3$ 26, and glucose 15 (300-305 mOsm) using a vibrating blade microtome (VT1200S, Leica Biosystems). The slices were transferred to the holding chamber and incubated in 34°C ACSF containing (in mM): NaCl 127, KCl 1.8, KH_2PO_4 1.2, $CaCl_2$ 2.4, $MgSO_4$ 1.3, $NaHCO_3$ 26, glucose 15, which was oxygenated with 95% O_2/5% CO_2 (300-305 mM). Forty-five minutes after recovery, the slices were then transferred into a recording chamber and perfused with oxygenated ACSF at 3 mL/min at 30-32°C. Whole-cell patch-clamp recordings were performed using glass pipettes with a resistance of 3-5 MΩ. A blue LED (475 nm; 10 mW/mm^2; UHP-Mic-LED-475; Prizmatix) was used to activate ChR2. The 475 nm light-evoked postsynaptic responses of NTS neurons were recorded in voltage-clamp mode using cesium (Cs^{2+})-based internal solution. The Cs^{2+}-based internal solution contained (in mM): $CsMeSO_3$ 130, $MgCl_2$ 1, $CaCl_2$ 1, HEPES 10, QX-314 2, EGTA 11, Mg-ATP 2, Na-GTP 0.3 (pH 7.3, ~295 mOsm). For the DREADD verification experiments, the resting membrane potential of $hM4Di^+$ neurons was recorded in current-clamp modes using

potassium-based internal solution containing (in mM) K-gluconate 130, $MgCl_2$ 1, $CaCl_2$ 1, KCl 1, HEPES 10, EGTA 11, Mg-ATP 2, Na-GTP 0.3 (pH 7.3, 290 mOsm). The locations of recorded NTS neurons were visualized with an air objective (4×; NA 0.13). EPSCs were recorded at a holding voltage of −70 mV, and IPSCs were recorded at a voltage of 0 mV. NBQX (Tocris, 1044; 10 μM) was used to block AMPA glutamate receptors. Picrotoxin (PTX; 1128 50 μM) was used to block $GABA_A$ receptors. The PPR was calculated by paired-pulse stimulation (1 ms; 50 ms interpulse intervals) as the ratio of the amplitude of the second response to that of the first.

QUANTIFICATION AND STATISTICAL ANALYSIS

Voltage clamp and current clamp recordings were carried out using a computer-controlled amplifier (MultiClamp 700B; Molecular Devices). During recordings, traces were low-pass filtered at 4 kHz and digitized at 20 kHz (DigiData 1550; Molecular Devices). Data were acquired with Axon Clampex 10.3 software. The amplitude and latency of postsynaptic currents (EPSCs or IPSCs) were manually measured from the averaged traces. EPSC and IPSC amplitudes were calculated as the difference between the peak amplitude in a predefined window after the light stimulation onset and the mean amplitude just before the EPSC or IPSC. EPSC or IPSC latency was measured as the time from the onset of light stimulation to the first intersection between the baseline and the EPSC or IPSC, which could be easily identified at the place of maximal rising/falling curvature. The EPSCs and IPSCs in our study sometimes showed multiple peaks, and we measured the latency of the first EPSC or IPSC. The jitter was defined as the standard deviation (SD) of the EPSC or IPSC onset latency across individual sweeps per cell (as least five sweeps per cell). Statistical analysis was performed using Igor Pro (Wavemetrics) and Prism (GraphPad Software). All statistical analyses were two-tailed comparisons. The data were analyzed using the Mann-Whitney test, Wilcoxon signed-rank test, two-way ANOVA, and paired t test. All data are expressed as the mean ± SEM. Difference between groups were considered statistically significant if $p < 0.05$.